PAPER

The Sharpless asymmetric aminohydroxylation reaction: optimising ligand/substrate control of regioselectivity for the synthesis of 3- and 4-aminosugars†

Jennifer A. Bodkin,[a] George B. Bacskay[a] and Malcolm D. McLeod*[a,b]

An investigation of the factors responsible for the sense and magnitude of regioselectivity in the Sharpless asymmetric aminohydroxylation (AA) has been conducted. Theoretical investigations of ligand–osmium binding geometry and experimental investigations of the Sharpless AA reaction on a series of functionalized pent-2-enoic acid ester substrates demonstrate that the opposite regioselectivity afforded using PHAL and AQN ligands results from a change in substrate orientation with respect to the catalyst. Two distinct ligand binding domains within the catalyst have been proposed that undergo attractive interactions with the substrates. Selective access to each of the four potential regio- and stereo-isomeric AA products could be achieved through the appropriate choice of ligand and substrate. These results have been applied toward the efficient stereoselective synthesis of naturally occurring and regioisomeric 3- and 4-aminosugar derivatives.

Introduction

The Sharpless asymmetric aminohydroxylation (AA) of alkenes has become a powerful catalytic asymmetric method for the synthesis of the vicinal amino alcohol functional array that has been applied to the construction of numerous biologically important targets.[1] Since it was first reported in 1996[2] the development of new nitrogen sources, new ligands, improved reaction conditions and a better under-standing of catalyst–substrate interactions have increased the scope and synthetic utility of the reaction.[3] However, the levels of selectivity obtained for some alkene substrates are not always high. The factors controlling regioselectivity are of particular interest as the issue of poor or unpredictable regioselectivity can be regarded as the greatest limiting factor in widespread application of the AA reaction in synthesis. Efforts to resolve this deficiency have included the development of the tethered aminohydroxylation (TA) reaction that gives secure regiochemical outcomes.[4] However, to date the TA reaction occurs without appreciable influence of chiral ligands and consequently has failed to give the same levels of enantioselectivity seen in the parent reaction.

A number of factors have been suggested to explain the regioselectivity observed in the AA reaction; these include alkene substitution, alkene polarization and ligand–substrate interaction.[3] Whilst it is difficult to assess these influences in isolation, it appears that ligand–substrate interactions have the greatest influence on regioselectivity.[3] In close analogy with the Sharpless asymmetric dihydroxylation (AD) reaction[5] the chiral ligands (Fig. 1) typically comprise two dihydroquinine (DHQ) or dihydroquinidine (DHQD) alkaloid units linked by an aromatic spacer unit such as phthalazine (PHAL) or anthraquinone (AQN). This ligand binds an imidotrioxoosmium species, to form the active catalytic species. Facial selectivity is governed by the diastereomeric alkaloid units DHQ and DHQD that give rise
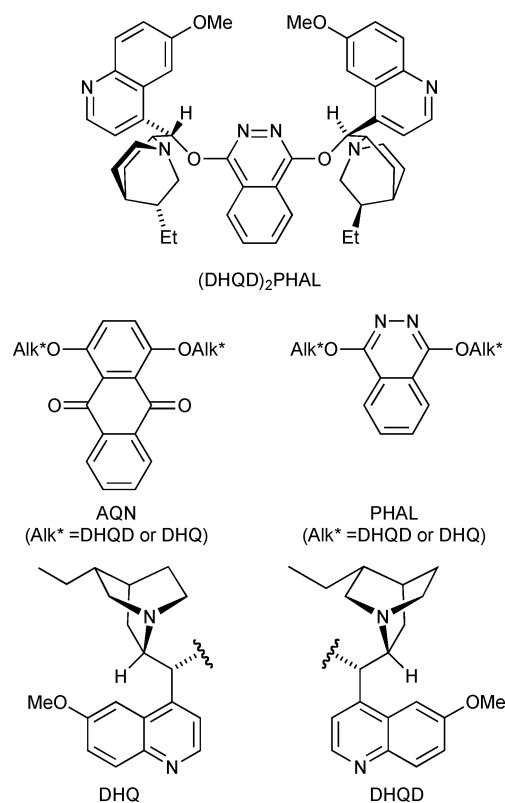

Fig. 1 Sharpless ligands.

[a]School of Chemistry, F11, University of Sydney, NSW, 2006, Australia
[b]Current Address: Research School of Chemistry, Australian National University, Canberra, ACT, 0200, Australia. E-mail: m.mcleod@rsc.chem.edu.au; Fax: +61 (0)2 6125 8114; Tel: +61 (0)2 6125 3504

† Electronic supplementary information (ESI) available: Experimental procedures, spectroscopic data, for compounds 9–23 and synthetic precursors, ^{1}H and ^{13}C NMR spectra for 12, 13 and 23, MOPAC input files for structures 4, 5, 6, 9e and 9f. See DOI: 10.1039/b803310b

to opposite enantiomers, a result that can be predicted by the Sharpless mnemonic.[3a–h,5] Compelling evidence for the role of the ligand on regioselectivity arises from the dramatic reversal of regioselectivity frequently observed when the aromatic spacer of the ligand is changed from PHAL to AQN.[1h–k,6–8] The role of the PHAL derived ligands has been explicitly considered by Janda[9] and Chuang,[10] who proposed that regioisomers in the AA reaction using PHAL ligands arise from two possible orientations of the substrate with respect to the ligand. Though it has been proposed that the change in ligand structure results in a change in substrate orientation with respect to the catalyst,[6a] the reasons for the dramatic reversal of regioselectivity observed for AQN derived ligands has not been fully elucidated.

In this paper we report theoretical investigations of ligand–osmium binding geometry and experimental investigations of the Sharpless AA reaction on a series of functionalized pent-2-enoic acid ester substrates that show that the opposite regioselectivity afforded using PHAL and AQN ligands results from a change in substrate orientation with respect to the catalyst. Two distinct ligand binding domains within the catalyst have been proposed that undergo attractive interactions with the substrates. The culmination of this study is the ability to access each of the four possible AA products selectively through the appropriate choice of ligand and substrate. As one illustration of its synthetic power, this AA methodology is applied towards the synthesis of naturally occurring and regioisomeric 3- and 4-aminosugar derivatives. This study expands previously reported attempts to exploit the AA reaction for the synthesis of amino sugar targets.[11]

Results and discussion

Consideration of how a change from PHAL to AQN ligands can favor two different regioisomers in the AA reaction of un-symmetrical alkenes leads to two proposed explanations. Firstly, assuming a fixed ligand–osmium binding geometry, a change in the substrate orientation with respect to the catalyst gives rise to different regioisomers of product (**1** *vs.* **2**, Scheme 1). A second and previously unexplored explanation is that changing the ligand spacer from PHAL to AQN leads to a change in ligand–osmium binding geometry. Based on this analysis the same approach of substrate with respect to the ligand also leads to the two regioisomeric products (**1** *vs.* **3**, Scheme 1).

As the starting point of the present study we conducted quantum chemical modeling on the imidotrioxoosmium complexes to identify preferred ligand binding geometries. The geometries of a range of structures were optimised,[12] followed by the calculation of zero point vibrational energies, by application of density functional theory utilizing the B3LYP functional[13,14] in conjunction with the 6–31G* basis set for carbon, nitrogen, oxygen and hydrogen, and the Stuttgart–Dresden relativistic effective core potential and SDD basis set[15] for osmium, collectively denoted here as 6–31G*. Single point energy calculations were then carried out with the inclusion of a set of 4f polarization functions ($\zeta = 0.55$) on osmium (denoted f/6–31G*). The calculations were performed using the Gaussian 98 programs.[16]

The computations started with uncomplexed $OsO_3NCOOMe$ **4** which is the simplest osmium species observed to participate in the AA reaction.[17] The optimised B3LYP/6–31G* structure **4** (Fig. 2) adopts a near ideal tetrahedral geometry with average N–Os–O
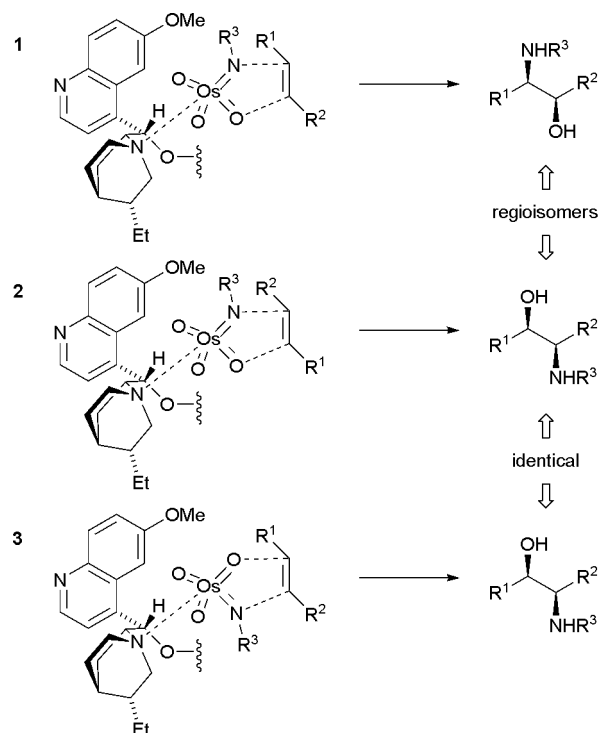
Scheme 1 Proposed explanations for the reversal of regioselectivity in the AA reaction of unsymmetrical alkenes: change in catalyst–substrate orientation **1** *vs.* **2**; or change in ligand–osmium geometry **1** *vs.* **3**.
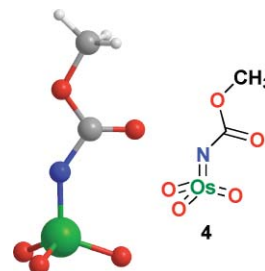

Fig. 2 Chem3D rendering of the B3LYP/6–31G* structure of $OsO_3NCOOMe$ **4**.

angles of 108.9°.[18] The imido substituent adopts a bent geometry with an Os–N–C angle of 143.9°.[19]

To determine the relative importance of different ligand–osmium geometries on catalyst structure, the effect of complex formation was investigated, with trimethylamine (NMe_3) selected to model the tertiary quinuclidine nitrogen atom of the ligand to which osmium binds (Scheme 2). Assuming idealized trigonal bipyramidal coordination, there are four possible structures and hence starting geometries **5–8** of the complex ($OsO_3NCOOMe.NMe_3$) as depicted in Scheme 2.

Geometry optimisation for structures **5** and **6** led to distinct local energy minima.[12] Complexes **7** and **8** converged to a **6**-like structure and were, therefore, eliminated from further consideration. The gas-phase energies using both basis sets (including zero point vibrational correction) show an energetic preference of 3.3 and 2.9 kcal mol^{−1} (6–31G*, f/6–31G*) for formation of complex **5** with two apical nitrogen substituents over complex **6** with an apical trimethylamine ligand and equatorial imido substituent. Solvation
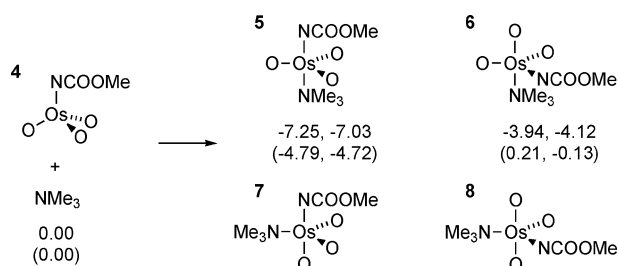
Scheme 2 Relative energies (B3LYP/6–31G*, f/6–31G* in kcal mol⁻¹) of amine–osmium complexation with the corresponding energies incorporating aqueous solvation treatment (COSMO) in brackets.

effects on the energetics were computed using the conductor-like screening model (COSMO)[20,21] with water as solvent. The results incorporating solvation were enlightening: there was an increase in energetic preference for formation of **5** over **6** (5.0 and 4.6 kcal mol⁻¹) reflecting a pronounced, relative destabilization of **6** upon solvation. The resulting, effectively zero, binding energies of +0.2 and −0.1 kcal mol⁻¹ for the formation of **6** suggest that this species is likely to be insignificant in the AA reaction medium.

The structure of the lowest energy osmium–ligand complex **5** obtained by the B3LYP/6–31G* calculations is shown in Fig. 3. The complex features apical nitrogen ligands in a distorted trigonal bipyramidal geometry (average imido N–Os–O angles of 102.3°) with the osmium lying out of the plane defined by the equatorial oxygen substituents and away from the apical NMe₃ ligand. The imido substituent adopts a bent geometry with an Os–N–C angle of 139.8°, marginally smaller than that of the uncomplexed species **4** (143.9°) and with a slightly longer Os–N bond length (1.78 Å *versus* 1.76 Å). The theoretically determined structure was compared with the reported crystal structure obtained from a related binuclear [OsO₃(N′Oct)]₂·DABCO complex containing *N*-alkylimido substituents.[22] The average imido Os–N bond length of 1.73 Å in the crystal structure is close to that observed in complex **5** (1.78 Å). The average Os–NMe₃ bond length of 2.45 Å in the crystal structure is of similar magnitude to that of the complex **5** (2.56 Å) and is consistent with weak complexation of the amine ligand to the osmium centre.[23] Shorter Os–NR₃ bond lengths (2.37–2.49 Å) are reported for the crystal structures of a number of OsO₄·NR₃ complexes[24–27] that contain an apical oxygen in the place of an imido substituent. The theoretical structure **5** contains
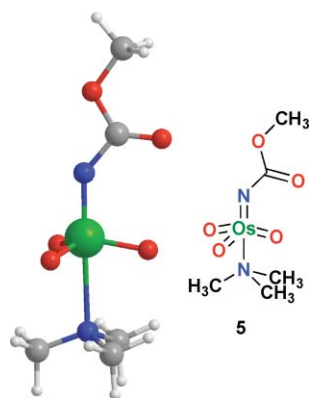

Fig. 3 Chem3D rendering of the B3LYP/6–31G* structure of the OsO₃NCOOMe·NMe₃ complex **5**.

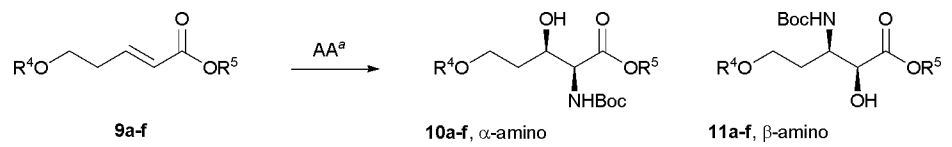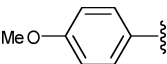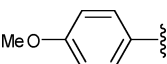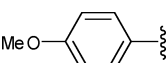similar equatorial Os–O bond lengths and angles to those observed in the reported crystal structures.[22–27]
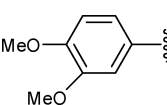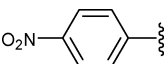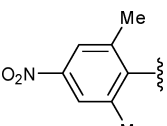
Atomic charges were computed from the natural bond order analysis[28] at the B3LYP/6–31G* level in aqueous solution. The atomic charge on the Os–N nitrogen (−0.555 a.u.) and Os–O oxygens (average −0.586 a.u.) are of similar magnitude. This finding is not consistent with a strong electronic influence on AA reaction regioselectivity involving the concerted [3 + 2] cycloaddition mechanism of complexes like **5** in the irreversible oxidation step.[29] In fact, the observed atomic charges suggest electronic effects would favour addition of the marginally more nucleophilic oxo-substituent to the electron deficient end of a polarised alkene π-bond in preference to the imido nitrogen. The above charges are not significantly different from the analogous gas phase values. It is worth noting also that the computed atomic charges are indicative of considerable semi-polar contribution to the Os–ligand bonds.

The significant energetic preference for osmium–ligand binding geometry **5** over **6** has implications for control of regioselectivity in the AA reaction. It is unlikely the changes to ligand structure would lead to significantly different osmium–ligand geometries as the osmium binds to a quinuclidine nitrogen of the alkaloid unit at some distance to the ligand PHAL or AQN spacer unit. Thus, our theoretical results support complex **5** as the favored osmium–ligand geometry and consequently imply that changes in regioselectivity arise due to changes in substrate–catalyst orientation (**1** *vs.* **2** in Scheme 1).

In order to empirically probe the hypothesis that substrate–catalyst orientation controls the regioselectivity of the AA reaction, the two possible binding modes (**1** and **2**, Scheme 1) were investigated by performing the AA reaction, using both PHAL and AQN derived ligands, on a range of 5-hydroxypent-2-enoic acid ester derivatives **9a–f** (Table 1). The substrate design allowed for variation of the substituents at the periphery that would not result in significant changes to substitution pattern, steric environment or electron demand of the reactive alkene. They were readily prepared by the sequence of Mitsunobu etherification[30] followed by cross metathesis,[31] which allowed variation of both aromatic ether and ester groups. All AA reactions were conducted under a standard set of reaction conditions using *tert*-butyl carbamate as the nitrogen source[32] and the commercially available 1,3-dichloro-5,5-dimethylhydantoin as oxidant.[33] Yields for PHAL derived ligands ranged from 56–81% and were generally higher than those derived from AQN ligands (30–75%).

As a starting point, the effect of increasing steric demand of the ester substituent (R⁵) was investigated. The AA reaction of **9a** (Table 1, entry 1) with (DHQD)₂PHAL derived catalyst gave high regioselectivity favoring the β-amino isomer **11a** with an enantiomeric excess of 96%. The use of (DHQ)₂PHAL ligands gave the enantiomeric product with similar levels of selectivity (entry 2). The good selectivity obtained with methyl ester **9a** correlated well with previous AA reactions of this substrate using ethyl carbamate[11] or bromoacetamide[9] variants of the AA reaction. The effect of increasing steric bulk of the ester (R⁵) was then investigated using *n*-butyl **9b** and *tert*-butyl **9c** substrates (entries 3, 4, 5). In these cases the PHAL ligands gave good regioselectivity (≥6 : 1) and excellent enantioselectivity (≥96% ee) for the β-amino isomer **11a–c** regardless of the ester group present. The minor regioisomers **10b** (4% ee) and **10c** (17% ee)

Table 1 Regio- and enantio-selectivity of the asymmetric aminohydroxylation reaction of 5-hydroxypent-2-enoic acid ester derivatives **9a–f**

Entry	Substrate	R^4	R^5	Alkaloid	PHAL		AQN	
					ratio α : β (**10** : **11**)	%ee (**11**)	ratio α : β (**10** : **11**)	%ee (**10**)
1	**9a**	MeO-phenyl	Me	DHQD	1 : 20	96	5 : 1	89
2	**9a**			DHQ^b	1 : 20	97	5 : 1	68
3	**9b**	MeO-phenyl	^{n}Bu	DHQD			2 : 1	87
4	**9b**			DHQ^b	1 : 9	99^c		
5	**9c**	MeO-phenyl	^{t}Bu	DHQ^b	1 : 6	96^d	1.2 : 1	51^e
6	**9d**^{f}	(MeO)$_2$-phenyl	Me	DHQD			7 : 1	93
7	**9d**^{f}			DHQ^b	1 : 15	98	7 : 1	92
8	**9e**	O$_2$N-phenyl	Me	DHQD	1 : 30	>95	8 : 1	Nd^g
9	**9e**			DHQ^b			7 : 1	>90
10	**9f**	Me,Me,O$_2$N-phenyl	Me	DHQD	1 : 3	93		
11	**9f**			DHQ^b			10 : 1	

^{a} Conditions: 5 mol% ligand, 5 mol% K$_2$OsO$_2$(OH)$_4$, ^{t}BuOCONH$_2$, 1,3-dichloro-5,5-dimethylhydantoin, NaOH, ^{n}PrOH/H$_2$O. ^{b} Enantiomeric products formed. ^{c} **10b** 4% ee. ^{d} **10c** 17% ee. ^{e} **11c** 74% ee. ^{f} Chlorination of the aromatic ring occurred to give the 2-chloro-4,5-dimethoxyphenyl ether products. ^{g} Not determined.

gave low enantioselectivity suggesting that the products did not result from effective substrate–catalyst interaction.

An understanding of the reaction substrate–catalyst interactions leading to this selectivity could be obtained by the inspection of CPK models. The geometry of the ligand was based on the reported X-ray crystal structure[34] while the geometry of the imidotrioxoosmium group with diapical nitrogen substituents was based on the results of 6–31G* structure calculations discussed above.[35] The structure of the catalyst is given in Fig. 4.

Given the favored osmium–ligand geometry predicted by the aforementioned modeling studies, it is proposed that selectivity for β-amino regioisomer arises from a preferred mode of binding in which the *p*-methoxyphenyl substituent[36] undergoes stabilizing aromatic-aromatic interactions with the face-to-face but offset methoxyquinoline rings of the catalyst (Fig. 5). This places the α- and β-alkene carbons in close proximity to the imido- and oxo-osmium substituents, respectively, leading to the formation of the β-amino regioisomers **11a–c** (Scheme 1, **1**, R^1 = CH$_2$CH$_2$OPMP, R^2 = COOR^5). The ester substituents lie in a relatively open region of the catalyst over the phthalazine spacer; an increase in the size of the ester substituent would be predicted to have little effect on the selectivity of the AA reaction.
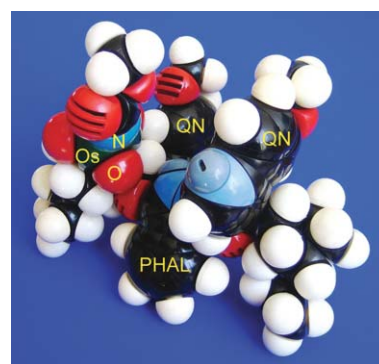
Fig. 4 Space-filling CPK model of the (DHQD)$_2$PHAL derived catalyst; PHAL = phthalazine, QN = methoxyquinoline.

The results obtained on the ester substrates **9a–c** with AQN ligands were very informative: the AA reaction of **9a** (entries 1–2) resulted in a reversal in regioselectivity to afford the α-amino isomer **10a** with 5 : 1 regioselectivity and moderate enantioselectivity. Increasing the size of the ester (R^5) from methyl to *tert*-butyl in substrates **9a–c** led to a complete erosion of

Fig. 5 Space-filling model of the (DHQD)₂PHAL derived catalyst with substrate **9a** docked in the proposed binding conformation; QN = methoxyquinoline unit, PMP = *p*-methoxyphenyl, α = alkene α-carbon, β = alkene β-carbon.

selectivity for the α-amino isomers **11a–c** as the size of the ester substituent increased.

A rationalization of these changes in AA regioselectivity could be obtained by inspection of CPK models of the AQN derived catalyst (Fig. 6). In this instance structural data for the AQN-derived ligands was not available so the geometry of ligand was provided by analogy with the PHAL crystal structure.[37,38] Inspection of the CPK model of the (DHQ)₂AQN catalyst highlights two key differences. The catalyst contains an extended aromatic spacer relative to the PHAL derived analogue. The catalyst also has a small but significant increase in steric crowding due to the replacement of the phthalazine nitrogens with the anthraquinone C–H groups.
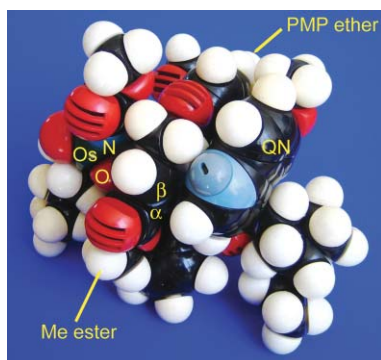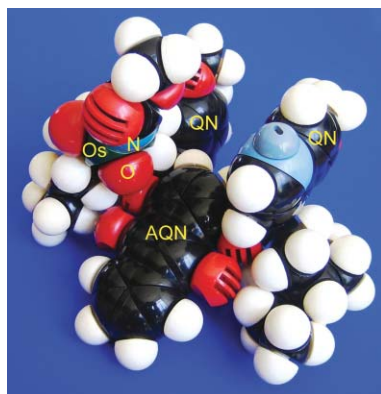

Fig. 6 Space-filling model of the (DHQD)₂AQN derived catalyst; AQN = anthraquinone unit, QN = methoxyquinoline unit.

The change in regioselectivity to favor the α-amino regioisomer **11a** is consistent with a change in alkene binding mode wherein the anthraquinone spacer of the catalyst interacts with the phenyl ether of the substrate. This opposite mode of binding places the places the α- and β-alkene carbons in close proximity to the oxo- and imido-osmium substituents, respectively, leading to the formation of the α-amino regioisomer (Scheme 1, **2**, R¹ = CH₂CH₂OPMP, R² = COOMe). This proposed mode of binding

is supported by the near complete erosion of selectivity for the α-amino isomer as the size of the ester substituent (R⁵) increases from Me to ⁿBu and ᵗBu in substrates **9a–c**, reflecting an increase in unfavourable steric interactions with the methoxyquinoline region of the catalyst. Poor catalyst–substrate interaction for the AA reaction of *tert*-butyl ester **9c** is also reflected by the low enantioselectivity (51% ee) of the α-amino product **11c**.

In a second series of experiments, the effect of altering the electronic properties of the aromatic ether was investigated through substrates **9a**, **d**, **e**. Substrates **9d** and **9e** gave excellent regio- and enantioselectivity for the β-amino isomer with PHAL ligands, indicative of a preferred mode of binding analogous to that proposed for PMP ether **9a** (Fig. 5), with the aromatic ether stabilized by the methoxyquinoline rings.[39]

Both substrates **9d** and **9e** containing, in relative terms, the electron rich 3,4-dimethoxyphenyl and electron poor *p*-nitrophenyl substituents, respectively, also gave improved regio- and enantioselectivity with AQN derived catalyst to afford a 7 : 1 and 7–8 : 1 ratio in favor of the α-amino isomer.[39,40] These results were initially surprising but could be rationalized by on the basis of the Hunter–Sanders model of π–π interactions.[41] Both face-to-face and edge-to-face interactions between the phenyl ether substituent and the anthraquinone spacer appear geometrically feasible for this system. For the case of face-to-face contacts, an increase in attractive π–π interactions could be afforded irrespective of the relative electron demand of the phenyl ether substituents, even, somewhat counter-intuitively, for those between the more electron deficient *p*-nitrophenyl substituent ring and anthraquinone units.[41] In contrast, attractive edge to face interactions based on electrostatic effects appear less reasonable in this system due to the π-deficient nature of the anthraquinone face unit and the varying electron demand of the edge aromatic substituents.[42–45] This proposition was confirmed by further work reported below that supports a face to face orientation of the aromatic moieties for these substrates.

Additional support for the two modes of binding was provided by the results of AA reaction of substrate **9f**. Incorporation of 2,6-dimethyl substitution changes the conformational preferences of the aryl ether **9f**.[46] The lowest energy conformation adopts a near 90° twist of the alkyl aryl ether carbon–oxygen bond, in contrast to the conformational preference of the 2,6-unsubstituted substrate **9e** (Scheme 3).[47] This twist of the aromatic ether **9f** would be expected to disrupt the normal mode of binding to the PHAL derived catalyst due to the increase in steric interference of the now orthogonal aromatic ether with the methoxyquinoline rings. In line with this expectation, the reaction of substrate **9f** gave only a 3 : 1 regioselectivity in favor of the β-amino regioisomer **10f**, a significant reduction from the 30 : 1 selectivity observed for the non-methylated counterpart **9e** (Table 1, entries 8 and 10). In contrast, the dimethylated substrate **9f** gave improved regioselectivity (10 : 1) for the α-amino isomer using AQN ligands (entries 8, 9 and 11). The proposed substrate–catalyst binding mode is depicted in Fig. 7. Significantly, the dimethyl substitution and twisting of the ring in substrate **9f** suggest face-to-face interaction between aryl ether and the extended aromatic spacer of the AQN ligand: the methyl groups render edge-on aromatic interaction unfavorable.

The trends in regioselectivity reported in this study are consistent with a binding model in which the ligand possesses two
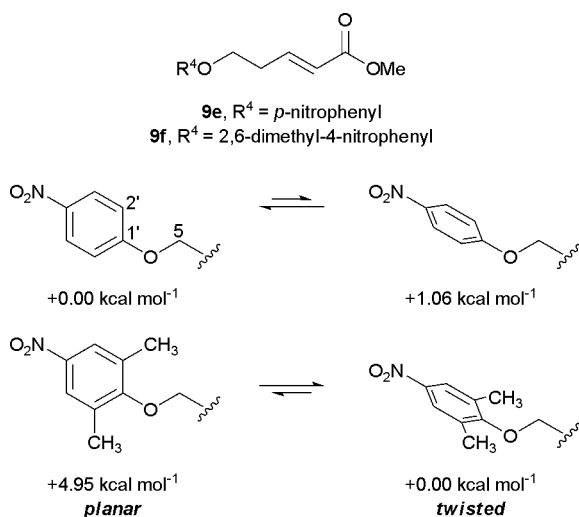
Scheme 3 Conformational preferences (C2′–C1′–O–C5) of phenyl ethers **9e** and **9f**.

9e, R^4 = *p*-nitrophenyl
9f, R^4 = 2,6-dimethyl-4-nitrophenyl

+0.00 kcal mol^{-1} +1.06 kcal mol^{-1}

+4.95 kcal mol^{-1} +0.00 kcal mol^{-1}
planar   *twisted*

N-Boc-L-acosamine **12**

15, R^6 = OMe, R^7 = Me
9e, R^6 = NO$_2$, R^7 = OMe

(DHQ)$_2$PHAL AA

(DHQ)$_2$AQN AA

13   *ent*-**10e**

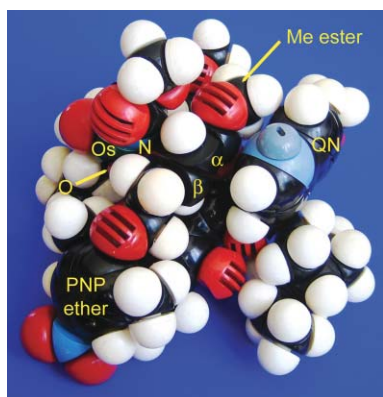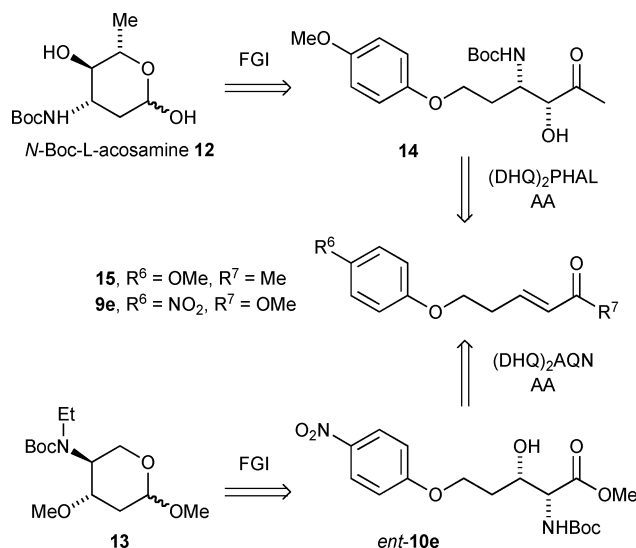**Scheme 4** Retrosynthetic analysis for 3- and 4-aminosugar targets.

Fig. 7 Space-filling model of the (DHQD)$_2$AQN derived catalyst with substrate **9f** docked in the proposed binding conformation; QN = methoxyquinoline unit, PNP = 2,6-dimethyl-4-nitrophenyl, α = alkene α-carbon, β = alkene β-carbon.

binding domains. The PHAL ligands favor interaction of the aryl ether (R^4) with the methoxyquinoline rings leading to formation of the β-amino product, whilst AQN ligands favor formation of the α-amino product *via* preferential interaction of the aryl ether with the extended AQN aromatic spacer. Application of this model through rational modification of the alkene substituents in concert with the appropriate ligand enables access to each of the four possible AA products with excellent enantio- and regio-selectivity. This study also provides insight into regiochemical preferences of other substate classes such as cinnamates[6] and styrenes,[7] and will assist in the design of future AA reaction processes.

Two amino sugar targets were selected to illustrate the utility of an AA-based methodology: the 3-amino sugar *N*-Boc-L-acosamine **12**, and the 4-amino sugar methyl-2,4-dideoxy-4-(*N*-Boc-ethylamino)-3-*O*-methyl-L-*threo*-pentopyranoside **13** (Scheme 4). Acosamine occurs in nature as both D- and L-isomeric forms as the carbohydrate component of the antibiotics actinoidin[48] (L-isomer) and *N*-acetylsporaviridin[49] (D-isomer),

and also a component of the chemotherapeutic agent 4′-epidoxorubicin (L-isomer).[50] Acosamine also serves as a key intermediate[51] in the synthesis of amino sugar components of the anthracycline antibiotics including daunomycin and adriamycin (L-daunosamine)[52] and from the pyranonaphthoquinone medermycin (D-angolosamine).[53] The 4-aminosugar **13** is an unusual 4-amino sugar component of calicheamicin γ$_1$^{1}, a member of the ene–diyne family of antibiotics.[54] The targets were chosen to highlight the flexibility of the AA reaction in accessing different regioisomers of the amino alcohol functionality.

The retrosynthetic analysis for the synthesis of these regioisomeric amino-sugar targets is given in Scheme 4. The 3-aminosugar *N*-Boc-L-acosamine **12** can be derived from the acyclic precursor **14** through a series of functional group interconversions. From the results of this work we anticipated that β-aminoketone precursor **14** could be derived from the α,β-unsaturated methyl ketone **15** through the agency of (DHQ)$_2$PHAL mediated AA reaction. Though the application of α,β-unsaturated ketone substrates such as **15** in the AA reaction was unprecedented, the observation that this catalyst system showed good tolerance for the changes in ester substitution with substrates **9a–c** gave confidence that such minor changes substrate would not unduly affect the proposed AA chemistry. The 4-aminosugar **13** could be synthesised from the previously described α-amino regioisomer **10e** through the stepwise introduction of the desired functionality.

Ketone **15** was prepared in two steps and 81% yield by Mitsunobu etherification of *p*-methoxyphenol and 3-butenol,[30] followed by cross metathesis of the resulting ether with methyl vinyl ketone.[31] Initial AA reactions using (DHQ)$_2$PHAL ligands and conventional conditions produced very low yields of the desired product **14**, and ^{1}H NMR spectroscopy indicated a major byproduct resulting from Michael addition of *tert*-butyl carbamate to the β-carbon of the unsaturated ketone **15**. When the AA reaction was buffered with 3 eq. NaHCO$_3$,[5] a 61% yield of the β-amino isomer **14** was produced with >15 : 1 regioselectivity and 90% ee (Scheme 5). Similarly, when pseudoenantiomeric (DHQD)$_2$PHAL ligand was used, a 63% yield of *ent*-**14** was
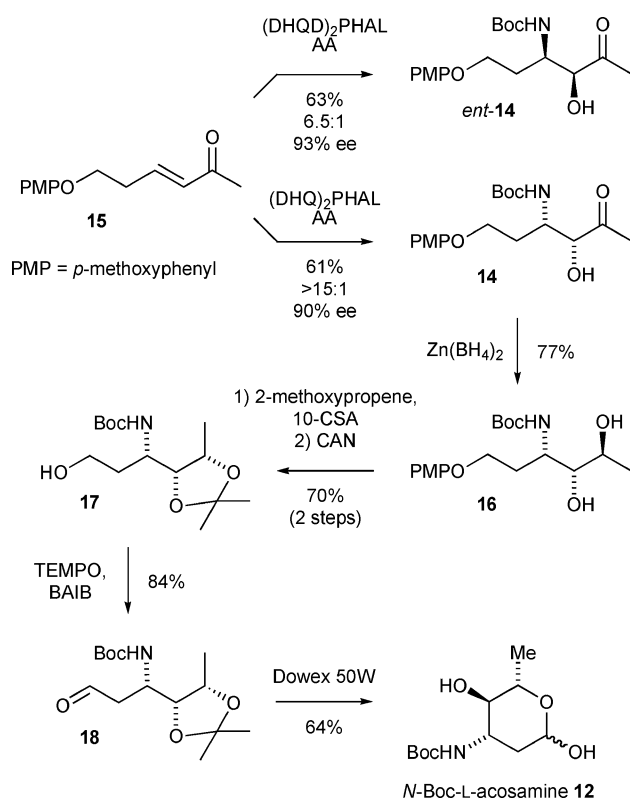
Scheme 5   Synthesis of *N*-Boc-L-acosamine **12**.

Scheme 6   Attempted synthesis of 4-aminosugar **13**.

produced with 6.5 : 1 regioselectivity for the β-amino isomer and an enantiomeric excess of 93%.

Reduction of the ketone **14** under conditions of chelation control[55] afforded amino diol **16** in 70% yield (Scheme 5), which was protected as the acetonide derivative. Confirmation of the *S*-configuration of the newly-formed secondary alcohol was obtained by ^{1}H NMR with the 6.6 Hz coupling constant between the protons of the acetonide ring, consistent with a *cis* relative stereochemistry.[56] Cleavage of the *p*-methoxyphenyl ether using ammonium cerium(IV) nitrate (CAN) afforded terminal alcohol **17** in two steps and 70% yield from diol **16**.[57] Oxidation of the primary alcohol **17** to aldehyde **18** was achieved using TEMPO–BAIB in 84% yield.[58] The final cyclisation step was performed using acidic resin DOWEX 50W[59] in aqueous dioxane to afford *N*-Boc-L-acosamine **12** ($[a_D] = -61$ (c 0.48, CH$_2$Cl$_2$)) in 6 steps and 18% overall yield from methyl ketone **15**. This route compares favorably in terms of synthetic efficiency with previous syntheses of acosamine **12**,[51,60a] and has the advantage of being equally applicable to the synthesis of D-acosamine through a single change of commercially available chiral ligand.

The 4-aminosugar **13**[60b–e] is regioisomeric to acosamine and incorporates alkyl substitution of the 3-hydroxyl and 4-amino groups. Although the synthesis of this functionalised target was ultimately frustrated, the attempted synthesis serves to highlight the potential of AA methodology to access regioisomeric 4-amino sugar precursors.

Methyl ester **9e**, containing *p*-nitrophenyl ether, has been shown to give selective formation of the correct α-amino regioisomer **10e** with AQN ligands in 75% yield, 7 : 1 regioselectivity and >90% ee (Table 1). The β-hydroxyl group was methylated using freshly
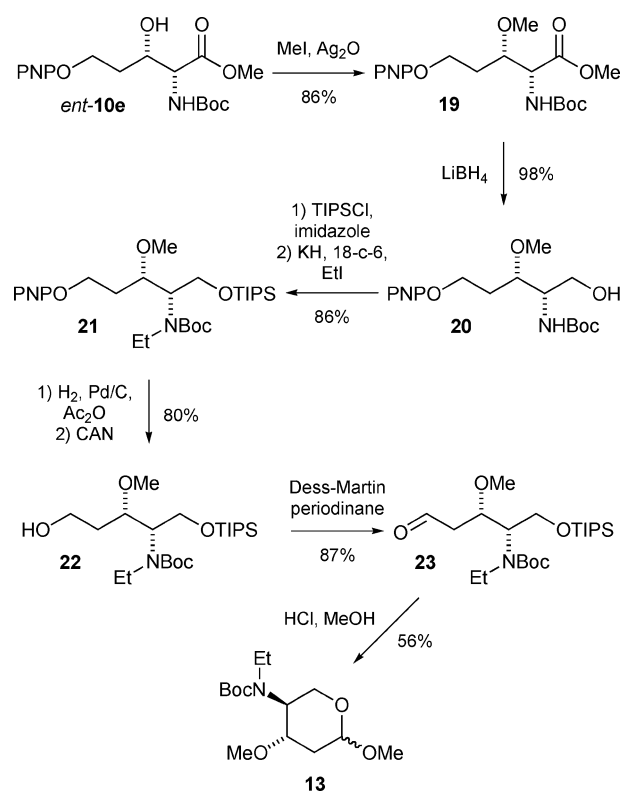
prepared silver(I) oxide and methyl iodide to afford methoxy compound **19** in 86% yield (Scheme 6).[61] Reduction of methyl ester **19** using lithium borohydride (98%) afforded the primary alcohol **20**.

Protection of primary alcohol **20** as the TIPS ether[62] was followed by *N*-ethylation, initially performed using potassium hydride, 18-crown-6 ether and iodoethane.[63] Thin layer chromatography indicated partial conversion to a single product **21**. However, the incomplete conversion prompted the addition of further potassium hydride and iodoethane, after which the formation of a byproduct became evident. Following purification, a 53% yield of desired product **21** was isolated, but a 42% yield of an *N*,*O*-diethylated compound was also produced, resulting from cleavage of the TIPS ether and ethylation of the resulting primary alcohol. Attempts with replacement of potassium hydride–18-crown-6 ether with various bases, including *n*-butyllithium, sodium hexamethyldisilazide or triethyloxonium tetrafluoroborate with butyllithium[64] were unsuccessful. On the assumption that superoxide contaminants in the potassium hydride reagent might be responsible for cleavage of the TIPS ether, purification of the potassium hydride reagent was conducted by the method of Macdonald and coworkers.[65] Using this purified reagent, the ethylation reaction proceeded smoothly to afford an 86% yield of the *N*-ethyl compound **21**.

Following this gratifying result, the next step was removal of the *p*-nitrophenyl ether. This was achieved in two steps in a modification of the procedure reported by Fukase.[66] Conversion of the nitro functionality to the amino derivative by hydrogenation in ethyl acetate, followed by reaction with acetic anhydride afforded the corresponding acetamide. Cleavage of the aromatic ether using

ammonium cerium(IV) nitrate under sodium bicarbonate-buffered conditions (to prevent cleavage of the TIPS ether) afforded alcohol **22** in 80% yield, which was oxidized using Dess–Martin periodinane[67] to afford the corresponding aldehyde **23** in 87% yield, providing the fully protected 4-aminosugar derivative in open chain form.

Unfortunately efforts to deprotect the TIPS ether **23** to afford the cyclic product **13** proved highly problematic. Treatment of aldehyde **23** with Dowex 50 W resin in both dioxane–water, conditions analogous to the used for the formation of *N*-Boc-L-acosamine **12**, or methanol, afforded only traces of what were tentatively identified as cyclic products. Treatment of aldehyde **23** with anhydrous methanolic hydrochloric acid at ambient temperatures effected removal of both TIPS ether and *N*-Boc protecting groups as indicated by ^{1}H NMR of the crude reaction mixture. However this product proved intractable to purification by chromatography on silica gel. Finally, treatment of aldehyde **23** with anhydrous methanolic hydrochloric at reduced temperature followed quenching the reaction *in situ* with triethylamine afforded a product (56%) that was tentatively identifed as a 2 : 1 mixture of methyl glycosides **13** with retention of the *N*-Boc protecting group. The formation of both the α- and β-anomeric methyl glycosides was indicated by their respective anomeric proton signals δ 4.74 (dd, J = 3.4, 1.5 Hz), 4.35 (1H, d, J = 8.0 Hz). The identity of the product was also supported by satisfactory LRMS and HRMS data. Unfortunately this material was observed to change during the acquisition of the overnight ^{13}C NMR data and this fact together limited access to stocks of the precursor aldehyde **23** rendered the complete characterization of this target impossible. Although the identity of this final amino sugar derivative could not be fully established, the chemistry illustrates the enantioselective AA based approach towards the synthesis of related 4-amino sugar targets.

Experimental

(2*R*,3*S*)-3-*tert*-Butoxycarbonylamino-2-hydroxy-5-(4-methoxy-phenoxy)pentanoic acid methyl ester *ent*-11a

General AA procedure 1 (substrate soluble in *n*-propanol): using (DHQ)₂PHAL

To a stirring solution of *tert*-butyl carbamate (0.747 g, 6.38 mmol, 3.0 eq.) in *n*-propanol (5 ml) at room temperature was added a solution of sodium hydroxide (0.254 g, 6.35 mmol, 3.0 eq.) in water (15 ml). To this mixture was added 1,3-dichloro-5,5-dimethylhydantoin (0.841 g, 4.27 mmol, 2.0 eq.), followed by a solution of (DHQ)₂PHAL (82.9 mg, 0.106 mmol, 5 mol%) in *n*-propanol (5 ml), then a solution of (2*E*)-5-(4-methoxy-phenoxy)pent-2-enoic acid methyl ester **9a** (0.503 g, 2.13 mmol) in *n*-propanol (5 ml). To this mixture was added potassium osmate dihydrate (39.0 mg, 0.106 mmol, 5 mol%). The resulting mixture was stirred at room temperature for 21 h, then quenched with sodium sulfite (2.19 g, 8.2 eq.), diluted with water (20 ml) and extracted into ethyl acetate (3 × 25 ml). The combined organic layers were dried, filtered and concentrated to afford a 20 : 1 mixture of regioisomers **11** : **10**. Purification by flash chromatography (column 1: 5% methanol–dichloromethane, column 2: 25% ethyl acetate–hexane) afforded pure *ent*-**11a** as a white solid (0.615 g,

78%, 97% ee (Chiralcel OD-H, 10% isopropyl alcohol–hexane: ret. time 22.3 (minor—**11a**) 35.4 (major—*ent*-**11a**) min)); mp 68–72 °C; $[a]_D$ = −67 (*c* 1.8, CH₂Cl₂); R_f 0.085 (25% ethyl acetate–hexane); ν_{max}/cm⁻¹ (thin film) 3369 (s, br, OH, NH), 1738 (s, C=O), 1713 (s, C=O); HRMS(EI) calc. for $C_{18}H_{27}NO_7$ 369.1788, found 369.1788; δ_H(400 MHz, CDCl₃) 6.81–6.71 (4H, m, 4 ArH), 4.80 (1H, d, J 9.5, NH), 4.29 (1H, br t (obs), J 7.1, C*H*(NH)), 4.25 (1H, s, C*H*(OH)), 4.00 (2H, t, J 6.0, OC*H₂*CH₂), 3.79 (3H, s, OCH₃), 3.76 (3H, s, OCH₃), 3.35 (1H, br s, OH), 2.12–1.99 (2H, m, OCH₂C*H₂*), 1.39 (9H, s, C(CH₃)₃); δ_C(100 MHz, CDCl₃) 173.9, 155.4, 153.9, 152.8, 115.7 (2C), 114.7 (2C), 79.7, 72.2, 65.6, 55.7, 52.8, 50.6, 31.9, 28.2 (3C); m/z(EI) 369 (M⁺, 83%), 296 ([M-OC(CH₃)₃]⁺, 41), 124 (100).

Further details of the experimental procedures and spectroscopic data in provided as ESI.†

Conclusions

A combinaton of theoretical and experimental investigation has been used to rationalise the different regiochemical outcomes associated with the AA reaction of pent-2-enoic acid ester substrates with either PHAL or AQN derived ligands. The synthesis of different amino alcohol regioisomers can be performed with high selectivity and the resulting products serve as useful building blocks for the synthesis of 3- and 4- amino sugar derivatives.

References

1 (*a*) G. Kim and N. Kim, *Tetrahedron Lett.*, 2007, **48**, 4481; (*b*) W. Kurosawa, H. Kobayashi, T. Kan and T. Fukuyama, *Tetrahedron*, 2004, **60**, 9615; (*c*) S. Singh and H. Han, *Tetrahedron Lett.*, 2004, **45**, 6349; (*d*) W. Kurosawa, T. Kan and T. Fukuyama, *J. Am. Chem. Soc.*, 2003, **125**, 8112; (*e*) H.-X. Zhang, P. Xia and W.-S. Zhou, *Tetrahedron*, 2003, **59**, 2015; (*f*) L. Dong and M. J. Miller, *J. Org. Chem.*, 2002, **67**, 4759; (*g*) C.-G. Yang, J. Wang, X.-X. Tang and B. Jiang, *Tetrahedron: Asymmetry*, 2002, **13**, 383; (*h*) B. Cao, H. Park and M. M. Joullie, *J. Am. Chem. Soc.*, 2002, **124**, 520; (*i*) C. E. Masse, A. J. Morgan, J. Adams and J. S. Panek, *Eur. J. Org. Chem.*, 2000, **14**, 2513; (*j*) C. E. Masse, A. J. Morgan and J. S. Panek, *Org. Lett.*, 2000, **2**, 2571; (*k*) J. S. Panek and C. E. Masse, *Angew. Chem., Int. Ed.*, 1999, **38**, 1093.
2 G. Li, H.-T. Chang and K. B. Sharpless, *Angew. Chem., Int. Ed. Engl.*, 1996, **35**, 451.
3 (*a*) H. C. Kolb, and K. B. Sharpless, in *Transition Metals for Organic Synthesis*, ed. M. Beller, and C. Bolm, Wiley-VCH, Weinheim, 2nd edn, 2004, ch. 2, p. 309; (*b*) K. Muniz-Fernandez, in *Transition Metals for Organic Synthesis*, ed. M. Beller, and C. Bolm, Wiley-VCH, Weinheim, 2nd edn, 2004, ch. 2, p. 326; (*c*) A. Bayer, in *Comprehensive Asymmetric Catalysis, Supplement*, ed. E. N. Jacobsen, A. Pfaltz, and H. Yamamoto, Springer, Berlin, 2004, ch. 2, p. 43; (*d*) D. Nilov, and O. Reiser, *Organic Synthesis Highlights V*, ed. H.-G. Schmalz, and T. Wirth, Wiley-VCH, Weinheim, 2003, p. 118; (*e*) D. Nilov and O. Reiser, *Adv. Synth. Catal.*, 2002, **344**, 1169; (*f*) J. A. Bodkin and M. D. McLeod, *J. Chem. Soc., Perkin Trans. 1*, 2002, 2733; (*g*) O. Reiser, *Angew. Chem., Int. Ed. Engl.*, 1996, **35**, 1308; (*h*) H. C. Kolb, and K. B. Sharpless, in *Transition Metals for Organic Synthesis*, ed. M. C. Beller and C. Bolm, Wiley-VCH, Weinheim, 1998, ch. 2, p. 243; (*i*) P. O'Brien, *Angew. Chem., Int. Ed.*, 1999, **38**, 326; (*j*) C. Bolm, J. P. Hildebrand, and K. Muniz, in *Catalytic Asymmetric Synthesis*, ed. I. Ojima, Wiley-VCH, New York, 2000, p. 399.
4 (*a*) T. J. Donohoe, P. D. Johnson, A. Cowley and M. Keenan, *J. Am. Chem. Soc.*, 2002, **124**, 12934; (*b*) T. J. Donohoe, P. D. Johnson and R. J. Pye, *Org. Biomol. Chem.*, 2003, **1**, 2025; (*c*) T. J. Donohoe, P. D. Johnson, R. J. Pye and M. Keenan, *Org. Lett.*, 2004, **6**, 2583; (*d*) M. N. Kenworthy, G. D. McAllister and R. J. K. Taylor, *Tetrahedron Lett.*, 2004, **45**, 6661; (*e*) M. N. Kenworthy and R. J. K. Taylor, *Org. Biomol. Chem.*, 2005, **3**, 603; (*f*) T. J. Donohoe, M. J. Chughtai, D. J. Klauber, D.

Griffin and A. D. Campbell, *J. Am. Chem.Soc.*, 2006, **128**, 2514; (*g*) T. J. Donohoe, C. J. R. Bataille, W. Gattrell, J. Kloesges and E. Rossignol, *Org. Lett.*, 2007, **9**, 1725; (*h*) K. L. Curtis, E. L. Evinson, S. Handa and K. Singh, *Org. Biomol. Chem.*, 2007, **5**, 3544.

5 H. C. Kolb, M. S. VanNieuwenhze and K. B. Sharpless, *Chem. Rev.*, 1994, **94**, 2483.

6 (*a*) B. Tao, G. Schlingloff and K. B. Sharpless, *Tetrahedron Lett.*, 1988, **39**, 2507; (*b*) H. Park, B. Cao and M. M. Joullie, *J. Org. Chem.*, 2001, **66**, 7223; (*c*) I. H. Kim and K. L. Kirk, *Tetrahedron Lett.*, 2001, **42**, 8401; (*d*) A. J. Morgan, C. E. Masse and J. S. Panek, *Org. Lett.*, 1999, **1**, 1949.

7 (*a*) The reversal of regioselectivity associated with styrenes and related substrates is less general: M. Bruncko, G. Schlingloff and K. B. Sharpless, *Angew. Chem., Int. Ed. Engl.*, 1997, **36**, 1483; (*b*) K. L. Reddy and K. B. Sharpless, *J. Am. Chem. Soc.*, 1998, **120**, 1207; (*c*) M. H. Haukaas and G. A. O'Doherty, *Org. Lett.*, 2001, **3**, 3899.

8 (*a*) A small reduction in the magnitude of regioselectivity has been observed on changing from (DHQ)₂PHAL to (DHQD)₂PHAL ligands in the aminohydroxylation of styrenes: P. J. O'Brien, S. A. Osborne and D. D. Parker, *J. Chem. Soc., Perkin Trans. 1*, 1998, 2519; (*b*) P. J. O'Brien, S. A. Osborne and D. D. Parker, *Tetrahedron Lett.*, 1998, **39**, 4099.

9 H. Han, C.-W. Cho and K. D. Janda, *Chem.–Eur. J.*, 1999, **5**, 1565.

10 (*a*) C.-Y. Chuang, V. C. Vassar, Z. Ma, R. Geney and I. Ojima, *Chirality*, 2002, **14**, 151; (*b*) C.-Y. Chuang, V. C. Vassar, Z. Ma, R. Geney and I. Ojima, *Chirality*, 2002, **14**, 757(erratum).

11 R. M. Davey, M. A. Brimble and M. D. McLeod, *Tetrahedron Lett.*, 2000, **41**, 5141.

12 Different conformations associated with the distinct geometries **4**, **5** and **6** were generated manually followed by full B3LYP/6–31G* geometry optimisation and frequency calculation to identify the corresponding equilibrium geometries.

13 A. D. Becke, *J. Chem. Phys.*, 1993, **98**, 5648.

14 C. Lee, W. Yang and R. G. Parr, *Phys. Rev. B*, 1988, **37**, 785.

15 D. Andrae, U. Haeussermann, M. Dolg, H. Stoll and H. Preuss, *Theor. Chim. Acta*, 1990, **77**, 123.

16 M. J. Frisch, G. W. Trucks, H. B. Schlegel, G. E. Scuseria, M. A. Robb, J. R. Cheeseman, V. G. Zakrzewski, J. A. Montgomery, Jr., R. E. Stratmann, J. C. Burant, S. Dapprich, J. M. Millam, A. D. Daniels, K. N. Kudin, M. C. Strain, O. Farkas, J. Tomasi, V. Barone, M. Cossi, R. Cammi, B. Mennucci, C. Pomelli, C. Adamo, S. Clifford, J. Ochterski, G. A. Petersson, P. Y. Ayala, Q. Cui, K. Morokuma, D. K. Malick, A. D. Rabuck, K. Raghavachari, J. B. Foresman, J. Cioslowski, J. V. Ortiz, A. G. Baboul, B. B. Stefanov, G. Liu, A. Liashenko, P. Piskorz, I. Komaromi, R. Gomperts, R. L. Martin, D. J. Fox, T. Keith, M. A. Al-Laham, C. Y. Peng, A. Nanayakkara, C. Gonzalez, M. Challacombe, P. M. W. Gill, B. G. Johnson, W. Chen, M. W. Wong, J. L. Andres, M. Head-Gordon, E. S. Replogle and J. A. Pople, *GAUSSIAN 98 (Revision A.7)*, Gaussian, Inc., Pittsburgh, PA, 1998.

17 M. Harding, J. A. Bodkin, C. A. Hutton and M. D. McLeod, *SYNLETT*, 2005, 2829.

18 MOPAC input files (6–31G*) for structures **4**, **5** and **6** are reported in the electronic supplementary information†.

19 The observation of this bent geometry is noteworthy, as a near linear geometry of related imidoosmium carbamates has been advanced to rationalize the empirically observed diastereoselectivity in the tethered aminohydroxylation reaction (ref. 4c). This model has recently been updated with the suggestion tethered aminohydroxylation occurs in the mechanistically distinct secondary cycle (ref. 4g).

20 C. J. Cramer and D. G. Truhlar, *Chem. Rev.*, 1999, **99**, 2161.

21 J. Tomasi and M. Persico, *Chem. Rev.*, 1994, **94**, 2027.

22 W. P. Griffith, N. T. McManus, A. C. Skapski and A. D. White, *Inorg. Chim. Acta*, 1985, **105**, L11.

23 For a review of imidoosmium compounds in organic synthesis see: K. Muniz, *Chem. Soc. Rev.*, 2004, **33**, 166.

24 A. J. Bailey, M. G. Bhowon, W. P. Griffithe, A. G. F. Shoair, A. P. White and D. J. Williams, *J. Chem. Soc., Dalton Trans.*, 1997, 3245.

25 E. J. Corey, M. C. Noe and S. Sarshar, *J. Am. Chem. Soc.*, 1993, **115**, 3828.

26 J. S. Svendsen, I. Marko, E. N. Jacobsen, C. Pulla Rao, S. Bott and K. B. Sharpless, *J. Org. Chem.*, 1989, **54**, 2263.

27 W. P. Griffith, A. C. Skapski, K. A. Woode and M. J. Wright, *Inorg. Chim. Acta*, 1978, **31**, L413.

28 (*a*) J. E. Carpenter and F. Weinhold, *J. Mol. Struct.*, 1988, **169**, 41; (*b*) J. E. Carpenter, *PhD thesis*, Unversity of Wisconsin, 1987; (*c*) J. P.

Foster and F. Weinhold, *J. Am. Chem. Soc.*, 1980, **102**, 7211; (*d*) A. E. Reed and F. Weinhold, *J. Chem. Phys.*, 1983, **78**, 4066; (*e*) A. E. Reed and F. Weinhold, *J. Chem. Phys.*, 1985, **83**, 1736.

29 For a detailed discussion on electronic effects and the mechanism of the Sharpless AA reaction see reference 3f and 23.

30 P. V. Ramachandran, J. S. Chandra and M. V. R. Reddy, *J. Org. Chem.*, 2002, **67**, 7547.

31 A. K. Chatterjee, T.-L. Choi, D. P. Sanders and R. H. Grubbs, *J. Am. Chem. Soc.*, 2003, **125**, 11360.

32 G. Li, H. H. Angert and K. B. Sharpless, *Angew. Chem., Int. Ed. Engl.*, 1996, **35**, 2813.

33 N. S. Barta, D. R. Sidler, K. B. Somerville, S. A. Weissman, R. D. Larsen and P. J. Reider, *Org. Lett.*, 2000, **2**, 2821.

34 W. Amberg, Y. L. Bennani, R. K. Chadha, G. A. Crispino, W. D. Davis, J. Hartung, K.-S. Jeong, Y. Ogino, T. Shibata and K. B. Sharpless, *J. Org. Chem.*, 1993, **58**, 844.

35 The imidotrioxoosmium unit was constructed at the University of Sydney workshop.

36 In this binding mode substrate adopts an s-*cis* conformation about the allylic C–C single bond. This conformation (C2–C3–C4–C5 dihedral angle 0°) is 0.64 kcal mol⁻¹ (MM2/Chem 3D Pro) higher in energy than the corresponding extended conformation (C2–C3–C4–C5 dihedral angle 121°). A similar conformation has been proposed for the Sharpless AD reaction of homoallyl aryl ethers. E. J. Corey, A. Guzman-Perez and M. C. Noe, *J. Am. Chem. Soc.*, 1995, **117**, 10805 and references cited therein.

37 We have been unable to grow crystals of the AQN ligands suitable for X-ray crystallography.

38 (*a*) A key torsion in the (DHDQ)₂PHAL ligands is the alkyl aryl ether (DHQD CH–O–C–N PHAL) that orients the DHQD alkaloid units relative to the PHAL spacer. In the (DHDQ)₂PHAL crystal structure this torsion approaches co-planarity (average 7.1°, ref. 34). Evidence for the same conformational preference for AQN derived ligands (DHQD CH–O–C–CH AQN) can be found by searching the Cambridge Structural Database for related alkyl aryl ethers based on the anthraquinone motif. Of the eleven structurally analogous torsions contained in six CSD structures; nine adopted a near coplanar torsions (average 5.99°) and two adopted out of plane torsions (76.0 and 98.9°); G. B. Caygill, D. S. Larsen and S. Brooker, *J. Org. Chem.*, 2001, **66**, 7427; (*b*) R. C. Cambie, R. M. Lorimer, C. E. F. Rickard and P. S. Rutledge, *Acta Crystallogr., Sect. C*, 1999, **55**, 436; (*c*) U. Siriwardane, S. P. Khanapure and E. R. Biehl, *Acta Crystallogr., Sect. C*, 1990, **46**, 924; (*d*) G. A. Sulikowski, E. Turos, S. J. Danishefsky and G. M. Shulte, *J. Am. Chem. Soc.*, 1991, **113**, 1373; (*e*) S. Norvez, F.-G. Tournilhac, P. Bassoul and P. Herson, *Chem. Mater.*, 2001, **13**, 2552; (*f*) H. Chikashita, J. A. Porco, Jr., T. J. Stout, J. Clardy and S. L. Schreiber, *J. Org. Chem.*, 1991, **56**, 1692.

39 The absolute configuration of both regioisomers **11e** and *ent*-**10e** was confirmed by the formation of *R*- and *S*- Mosher's esters and application of the modified Mosher's method: I. Ohtani, T. Kusumi, Y. Kashman and H. Kakisawa, *J. Am. Chem. Soc.*, 1991, **113**, 4092.

40 The *para*-nitrophenyl ether also leads to improved regioselectivity in the AA reaction of related mono-substituted alkene substrates (ref. 16).

41 C. A. Hunter and J. K. M. Sanders, *J. Am. Chem. Soc.*, 1990, **112**, 5525.

42 E. A. Meyer, R. K. Castellano and F. Diederich, *Angew. Chem., Int. Ed.*, 2003, **42**, 1210.

43 J. B. Jennings, B. M. Farrel and J. M. Malone, *Acc. Chem. Res.*, 2001, **34**, 885.

44 (*a*) F. J. Carver, C. A. Hunter, D. J. Livingstone, J. F. McCabe and E. M. Seward, *Chem.–Eur. J.*, 2002, **8**, 2847; (*b*) F. J. Carver, C. A. Hunter, P. S. Jones, D. J. Livingstone, J. F. McCabe, E. M. Seward, P. Tiger and S. E. Spey, *Chem.–Eur. J.*, 2001, **7**, 4854.

45 (*a*) S. Paliwal, S. Geib and C. S. Wilcox, *J. Am. Chem. Soc.*, 1994, **116**, 4497; but see also; (*b*) E. Kim, S. Paliwal and C. S. Wilcox, *J. Am. Chem. Soc.*, 1998, **120**, 11192; (*c*) K. Nakamura and K. N. Houk, *Org. Lett.*, 1999, **1**, 2049.

46 The planar conformation (C2′–C1′–O–C5 constrained dihedral angle 0°, local maximum) of the aryl ether in **9f** is 4.95 kcal mol⁻¹ higher in energy (MM2/Chem3D Pro) than the corresponding twisted conformation (C2′–C1′–O–C5 dihedral angle 76°, local minimum). The MOPAC input file of structure **9f** is reported in the electronic supplementary information†.

47 The planar conformation (C2′–C1′–O–C5 dihedral angle 0°, local minimum) of the aryl ether in **9e** is 1.06 kcal mol⁻¹ lower in energy

(MM2/Chem3D Pro) than the corresponding twisted conformation (C2′–C1′–O–C5 dihedral angle 84°, local minimum). The MOPAC input file for structure **9e** is reported in the electronic supplementary information†.

48 (*a*) N. N. Lomhna, I. A. Spiridonova, Y. N. Sheinker and T. F. Vlasova, *Khim. Prir. Soedin.*, 1973, **9**, 101; (*b*) I. A. Spiridonova, M. S. Yurina, N. N. Lomakina, F. Sztaricskai and F. Bognar, *Antibiot. Med. Biotekhnol.*, 1976, **21**, 304.

49 K.-I. Harada, S. Ito and M. Suzuki, *Carbohydr. Res.*, 1979, **75**, C17.

50 A. C. Weymouth-Wilson, *Nat. Prod. Rep.*, 1997, **14**, 99.

51 F. M. Hauser and S. R. Ellenberger, *Chem. Rev.*, 1986, **86**, 35.

52 F. Arcamone, G. Cassinelli, P. Orezzi, G. Franceschi and R. Mondelli, *J. Am. Chem. Soc.*, 1964, **86**, 5335.

53 M. Brufani and W. Keller-Scherlein, *Helv. Chim. Acta*, 1966, **49**, 1962.

54 M. D. Lee, T. S. Dunne, M. M. Siegel, C. C. Chang, G. O. Morton and D. B. Borders, *J. Am. Chem. Soc.*, 1987, **109**, 3464.

55 W. J. Gensler, F. A. Johnson and D. B. Sloan, *J. Am. Chem. Soc.*, 1960, **82**, 6074.

56 (*a*) J. R. Vyvyan, J. A. Meyer and K. D. Meyer, *J. Org. Chem.*, 2003, **68**, 9144; (*b*) T. R. Hoye, J. I. Jimenez and W. T. Shier, *J. Am. Chem. Soc.*, 1994, **116**, 9409.

57 T. Fukuyama, A. A. Laird and L. M. Hotchkiss, L. M., *Tetrahedron Lett.*, 1985, **26**, 6291.

58 T. M. Hansen, G. J. Florence, P. Lugo-Mas, J. Chen, J. N. Abrams and C. J. Forsyth, *Tetrahedron Lett.*, 2003, **44**, 57.

59 K. H. Park, Y. J. Yoon and S. G. Lee, *Tetrahedron Lett.*, 1994, **35**, 9737.

60 (*a*) K. J. Fraunhoffer and M. C. White, *J. Am. Chem. Soc.*, 2007, **129**, 7274; (*b*) K. C. Nicolaou, R. D. Groneberg, T. Miyazaki, N. A. Stylianiedes, T. J. Schulze and W. Stahl, *J. Am. Chem. Soc.*, 1990, **112**, 8193; (*c*) W. R. Roush and J. A. Hunt, *J. Org. Chem.*, 1995, **60**, 798; (*d*) D. Kahne, D. Yang and M. D. Lee, *Tetrahedron Lett.*, 1990, **31**, 21; (*e*) R. D. Groneberg, T. Miyazaki, N. A. Stylianiedes, T. J. Schulze, W. Stahl, E. P. Schreiner, T. Suzuki, Y. Iwabuchi, A. L. Smith and K. C. Nicolaou, *J. Am. Chem. Soc.*, 1993, **115**, 7593.

61 N. Finch, J. J. Fitt and I. H. S. Hsu, *J. Org. Chem.*, 1975, **40**, 206.

62 R. F. Cunico and L. Bedell, *J. Org. Chem.*, 1980, **45**, 4797.

63 R. T. Shuman, E. L. Smithwick, D. L. Smiley, G. S. Brooke, and P. D. Gesellchen, in *Pept.: Struct. Funct., Proc. Am. Pept. Symp., 8th edn*, ed. V. J. R. Hruby and H. Daniel, Pierce Chem. Co., Rockford, III, 1983, p. 143.

64 D. W. Hansen, Jr. and D. Pilipauskas, *J. Org. Chem.*, 1985, **50**, 945.

65 T. L. Macdonald, J. Natalie, J. Kenneth, G. Prasad and J. S. Sawyer, *J. Org. Chem.*, 1986, **51**, 1124.

66 K. Fukase, T. Yasukochi, Y. Nakai and S. Kusumoto, *Tetrahedron Lett.*, 1996, **37**, 3343.

67 D. B. Dess and J. C. Martin, *J. Am. Chem. Soc.*, 1991, **113**, 7277.